JOC The Journal of Organic Chemistry

Note

pubs.acs.org/joc

Predicting and Understanding the Reactivity of Aza[60]fullerenes

Yago García-Rodeja,[†] Miquel Solà,[‡] and Israel Fernández*[,†]

[†]Departamento de Química Orgánica I, Facultad de Ciencias Químicas, Universidad Complutense de Madrid, 28040-Madrid, Spain

[‡]Institut de Química Computacional i Catàlisi and Departament de Química, Universitat de Girona, Campus Montilivi, 17003-Girona, Spain

Supporting Information

ABSTRACT: The Diels–Alder reactivity of $C_{59}NH$ azafullerene has been explored computationally. The regioselectivity of the process and the factors controlling the reduced reactivity of this system with respect to the parent C_{60} fullerene have been analyzed in detail by using the activation strain model of reactivity and the energy decomposition analysis method. It is found that the presence of the nitrogen atom and the CH fragment in the fullerene reduces the interaction between the deformed reactants along the entire reaction coordinate.

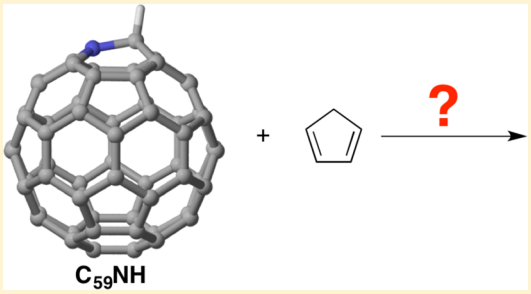

Due to their numerous potential applications in materials science and medicinal chemistry, fullerenes have become a highly valuable molecular species.[1] For this reason, it is not surprising that since the discovery of the parent C_{60}-fullerene,[2] a good number of synthetic methods have been developed to produce new fullerene derivatives with tunable properties.[3] In sharp contrast, the chemistry of heterofullerenes, i.e. fullerenes where carbon atoms of the cage are replaced by heteroatoms, is comparatively underdeveloped. This is mainly due to the difficulties associated with the preparation of such species. Indeed, most of the known heterofullerenes have only been prepared in the gas phase and detected by mass spectrometry.[4]

In this sense, azafullerenes constitute the only class of heterofullerenes which have been synthesized in macroscopic quantities. For instance, monoazafullerenes $C_{59}N$ and $C_{69}N$ were isolated as the stable dimers $(C_{59}N)_2$ and $(C_{69}N)_2$, respectively,[5] and very recently also as their corresponding endohedral species $(H_2O@C_{59}N)_2$ and $(H_2@C_{59}N)_2$.[6] In addition, the azafullerene derivatives $C_{59}NH$ and $C_{59}NR_5$ have been also obtained on a preparative scale.[7,8] Because of their exceptional energy- and charge-transfer properties, $C_{59}N$-based donor–acceptor dyads were employed in organic solar cells.[7c,9] In this context, it would be highly desirable to understand the factors which control the reactivity of these particular heterofullerenes to produce novel azafullerene derivatives that could be used in the design of more efficient solar cells.

In recent years, we have applied computational methods to predict and gain a deeper insight into the reactivity of fullerenes.[10] In this regard, by means of the so-called Activation Strain Model (ASM)[11] of reactivity in combination with the Energy Decomposition Analysis (EDA) method,[12] we were very recently able to fully understand those factors governing the reactivity of fullerenes and related species.[13] The insight gained has allowed us not only to understand the reactivity of these systems in a quantitative manner but also to guide future experimental developments in the chemistry of fullerenes. Herein, we are interested in further understanding the reactivity of azafullerenes, which is almost completely unexplored to date.[14] To this end, we have selected the Diels–Alder (DA) reaction between hydroazafullerene $C_{59}NH$ and cyclopentadiene (CP).

In contrast to the parent C_{60}-fullerene, where the preferred [6,6]-pyracylenic bonds are equivalent within the entire cage, $C_{59}NH$ exhibits 16 chemically different [6,6]-bonds (Figure 1). In addition, two possible isomers per [6,6]-bond can be produced in the DA reaction. Our calculations indicate that the

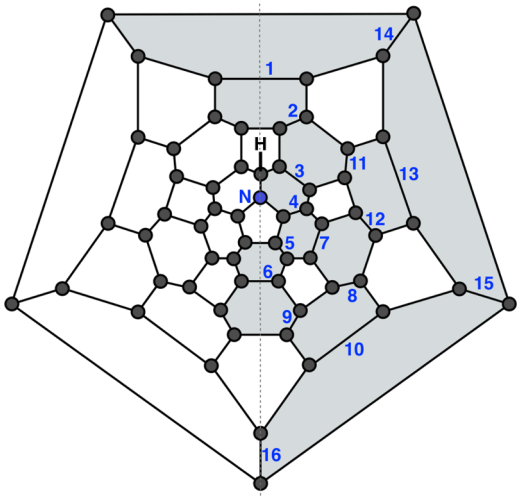

Figure 1. [6,6]-Bonds in $C_{59}NH$ considered in this study.

Received: October 5, 2016
Published: December 7, 2016

DOI: 10.1021/acs.joc.6b02424
J. Org. Chem. 2017, 82, 754–758

Table 1. Computed Relative Energies (in kcal/mol, at the BP86-D3/TZ2P+//RI-BP86-D3/def2-SVP level) and Free Energies (within Parentheses, at the RI-BP86-D3/def2-SVP Level) for the Diels−Alder Cycloaddition Reactions between CP and $C_{59}NH$ and C_{60} on [6,6]-Pyracylenic Bonds

[6,6]-bond	ΔE_{RC}[a]	$\Delta E^{\ddagger}$[b]	ΔE_R[c]	$\Delta\Delta E_{TS}$[d]	$\Delta\Delta E_R$[e]
1	−7.4 (2.8)	8.3 (12.6)	−19.9 (−7.0)	0.4 (0.8)	1.9 (1.8)
2	−7.2 (2.8)	10.0 (13.9)	−16.8 (−4.2)	2.0 (2.1)	5.1 (4.6)
3	**−7.9 (1.8)**	**8.0 (11.8)**	**−21.8 (−8.8)**	**0.0 (0.0)**	**0.0 (0.0)**
4	−6.4 (3.2)	10.1 (14.7)	−19.2 (−6.5)	2.1 (2.9)	2.6 (2.3)
5	−7.1 (3.0)	9.2 (13.4)	−15.3 (−2.7)	1.2 (1.5)	6.5 (6.1)
6	−7.4 (2.9)	8.5 (12.7)	−19.6 (−6.7)	0.5 (0.9)	2.2 (2.0)
7	−6.4 (3.3)	11.6 (16.3)	−14.3 (−1.8)	3.6 (4.4)	2.2 (7.0)
8	−6.8 (3.2)	9.6 (14.1)	−17.4 (−4.7)	1.6 (2.2)	7.5 (4.1)
9	−7.3 (2.6)	8.2 (13.4)	−19.5 (−6.8)	0.2 (0.5)	4.5 (2.0)
10	−7.2 (2.9)	8.9 (13.1)	−18.4 (−5.7)	0.9 (1.2)	2.3 (3.1)
11	−6.6 (3.3)	11.0 (15.6)	−14.6 (−2.1)	3.0 (3.8)	7.2 (6.7)
12	−7.2 (2.9)	8.4 (12.6)	−19.0 (−6.3)	0.4 (0.7)	2.8 (2.5)
13	−7.0 (3.1)	9.2 (13.6)	−17.6 (−5.1)	1.2 (1.7)	4.2 (3.7)
14	−7.2 (2.8)	8.4 (12.7)	−19.0 (−6.3)	0.4 (0.9)	2.8 (2.5)
15	−7.0 (3.0)	8.9 (13.3)	−18.1 (−5.5)	0.9 (1.5)	3.7 (3.3)
16	−7.2 (2.9)	9.4 (13.8)	−17.6 (−4.9)	1.5 (2.0)	4.2 (3.9)
C_{60}[f]	−7.1	5.2[g]	−23.4[g]		

[a]Reactant complex (**RC**) energy: $\Delta E_{RC} = E(\mathbf{RC}) - E(C_{59}NH) - E(CP)$. [b]Activation energy: $\Delta E^{\ddagger} = E(\mathbf{TS}) - E(\mathbf{RC})$. [c]Reaction energy: $\Delta E_R = E(\text{cycloadduct}) - E(C_{59}NH) - E(CP)$. [d]$\Delta\Delta E_{TS} = \Delta E^{\ddagger}(\mathbf{TS}_i) - \Delta E^{\ddagger}(\mathbf{TS3})$. [e]$\Delta\Delta E_R = \Delta E_R(\text{bond i}) - \Delta E_R(\text{bond 3})$. [f]Data taken from ref 13a (computed at the same level of theory). [g]Experimental values of activation energy and reaction energy are 6.9 and −19.8 kcal/mol, respectively.[16a]

barrier and reaction energy differences between both approaches are negligible (<0.5 kcal/mol), and therefore, below we only refer to the most favored approach.[15]

Similar to the reaction profile computed for C_{60},[13a] in all cases the reaction proceeds with the formation of an initial reactant complex (**RC**) which lies ca. −7.0 kcal/mol below the separate reactants (see Table 1). The occurrence of this stable van de Waals complex highlights the importance of including dispersion corrections in the calculations involving fullerenes, as suggested previously by us.[13,16] From this species, a concerted and relatively synchronous [4 + 2]-cycloaddition reaction takes place (see the corresponding fully optimized transition states in the Supporting Information) to produce the respective [6,6]-cycloadduct in a highly exothermic reaction (ΔG_R ca. −18 kcal/mol).

According to the data gathered in Table 1, the DA reaction with CP occurs preferentially, both kinetically and thermodynamically, on [6,6]-bond 3, which belongs to the six-membered ring where the nitrogen atom is present.[17] Interestingly, the computed energies clearly indicate that the DA reactivity of the azafullerene $C_{59}NH$ is lower than that of C_{60} but higher than that of prototypical dienophiles, from both kinetic and thermodynamic points of view.[18] This finding becomes evident when comparing the barrier and reaction energies computed for the process involving the [6,6]-bond 16, i.e. the farthest bond to the nitrogen atom thus resembling the [6,6]-bond of C_{60}, which are also higher than those computed for the process involving C_{60}. This suggests that the heterocyclic ring in $C_{59}NH$ strongly influences not only the rings close to it but also the entire fullerenic cage. It is also worthy to note that the regioselectivity of the DA in $C_{59}NH$ is expected to be low since there are five bonds (1, 6, 9, 12, and 14) with barriers less than 0.5 kcal/mol higher than the addition with the lowest energy barrier (3).

Although the reduced reactivity of $C_{59}NH$ may be initially related to the slight destabilization of the corresponding LUMO (−4.26 eV vs −4.20 eV, for C_{60} and $C_{59}NH$, respectively), the Activation Strain Model (ASM)[11] of reactivity was applied next to gain a quantitative understanding of the origins of this reactivity trend. Within the ASM, also known as the *distortion/interaction model*,[19] the potential energy surface $\Delta E(\zeta)$ is decomposed along the reaction coordinate ζ into two main contributions, namely the strain energy, $\Delta E_{strain}(\zeta)$, plus the interaction energy, $\Delta E_{int}(\zeta)$ (eq 1). Whereas the ΔE_{strain} term is associated with the energy required to deform the individual reactants from their equilibrium geometries, the ΔE_{int} term measures the interaction between the deformed reactants as they approach each other.

$$\Delta E(\zeta) = \Delta E_{strain}(\zeta) + \Delta E_{int}(\zeta) \quad (1)$$

Figure 2 illustrates the computed activation strain diagrams (ASD) for the cycloaddition reactions involving CP and C_{60} (solid lines) and $C_{59}NH$ (bond 3, dotted lines; bond 7, dashed lines) from the respective reactant complexes up to the corresponding transition states. The shapes of the different curves are rather similar in both cases. Thus, the interaction energy between the deformed reactants, measured by the ΔE_{int} term, remains practically constant at the beginning of the reaction mainly due to the onset of overlap and Pauli repulsion between the occupied π orbitals on either of the reactants. Then, the ΔE_{int} term inverts at a certain point along the reaction coordinate (i.e., at forming C···C distances of ca. 2.5 Å) and becomes increasingly more stabilizing when reaching the corresponding transition state region. Similar behavior was found in related DA reactions[13,20] as well as in different types of pericyclic reactions.[21] Nevertheless, the strong destabilizing effect of the deformation energy required to adopt the transition state geometry (ΔE_{strain}) overcomes the stabilization provided by the interaction term and therefore becomes the major factor controlling the activation barrier of the process.

Despite that, the strain energy is not the physical factor responsible for the different reactivity of C_{60} and $C_{59}NH$. As clearly seen in Figure 2, the computed strain terms are rather similar for both cycloaddition reactions, and even less

DOI: 10.1021/acs.joc.6b02424
J. Org. Chem. 2017, 82, 754−758

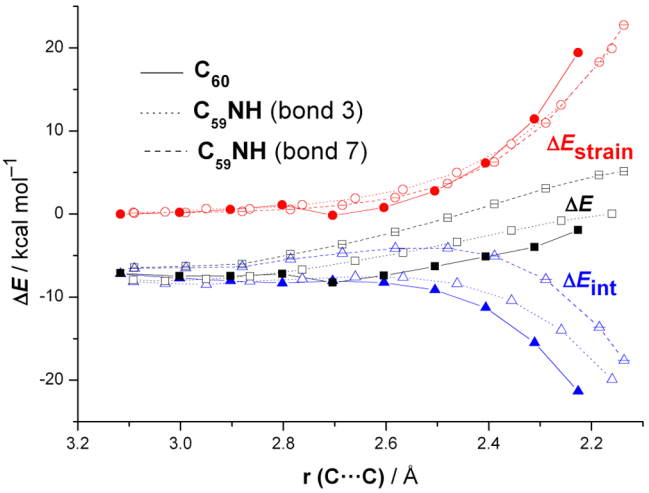

Figure 2. Comparative activation-strain diagrams for the Diels–Alder reactions between CP and C_{60} (solid lines), $C_{59}NH$ (bond 3, dotted lines), and $C_{59}NH$ (bond 7, dashed lines) along the reaction coordinate projected onto the shortest forming C···C bond distance. All data have been computed at the ZORA-BP86-D3/TZ2P+//RI-BP86-D3/def2-SVP level.

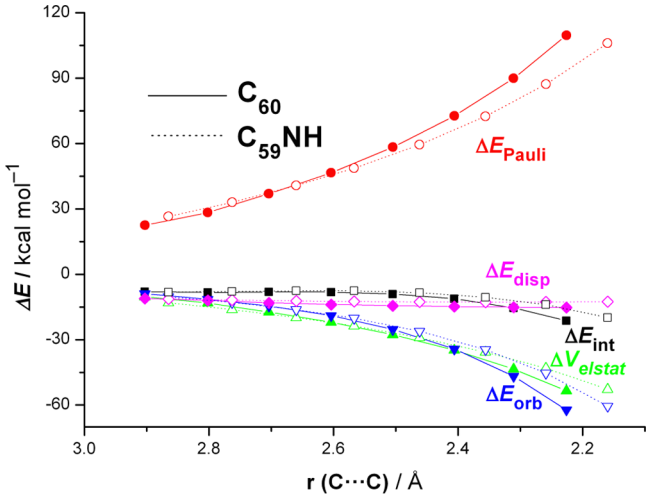

Figure 3. Decomposition of the interaction energy for the [4 + 2]-cycloaddition reactions between CP and C_{60} (solid lines) and $C_{59}NH$ (bond 3, dotted lines) along the reaction coordinate projected onto the shortest forming C···C bond distance. All data have been computed at the ZORA-BP86-D3/TZ2P+//RI-BP86-D3/def2-SVP level.

destabilizing for the less reactive azafullerene system at the transition state region. At variance, the interaction energy between the deformed reactants is markedly stronger for the reaction involving C_{60} as compared to $C_{59}NH$. Therefore, it can be concluded that the interaction energy constitutes the main factor governing the different reactivity of these fullerenes. For instance, at the same C···C forming distance of 2.3 Å, the difference in the interaction energy $\Delta\Delta E_{int}$ = 3.7 kcal/mol roughly matches the total energy difference between both transformations ($\Delta\Delta E$ = 2.4 kcal/mol). The major role of the interaction energy in the process becomes evident when considering the ASD for the reaction involving the least reactive [6,6]-bond of $C_{59}NH$ (bond 7, dashed lines in Figure 2). Indeed, for this particular reaction, the strain energy is nearly identical to that computed for the most reactive bond 3. However, the interaction energy between the deformed reactants is clearly weaker along the entire reaction coordinate, and as a result, the computed activation barrier for this process is much higher.

Further quantitative insight into the factors making the interaction between the reactants weaker for the process involving the azafullerene system can be gained by means of the Energy Decomposition Analysis (EDA) method.[12] Within this method, the ΔE_{int} term can be partitioned into meaningful energy contributions (eq 2), namely the Pauli repulsion (ΔE_{Pauli}, which comprises the closed-shell repulsion between filled orbitals), ΔV_{elstat} term (which corresponds to the classical Coulombic/electrostatic attraction and repulsion between electrons and nuclei), the orbital interaction (ΔE_{orb}, which accounts for electron-pair bonding, charge transfer, and polarization), and the ΔE_{disp} term, which takes into account the interactions which derive from dispersion forces. Therefore:

$$\Delta E_{int}(\zeta) = \Delta E_{Pauli}(\zeta) + \Delta V_{elstat}(\zeta) + \Delta E_{orb}(\zeta) + \Delta E_{disp}(\zeta) \quad (2)$$

Figure 3 graphically shows the evolution of the different contributions to the total interaction energy for the cycloaddition reactions involving C_{60} (solid lines) and $C_{59}NH$ (bond 3, dotted lines) along the reaction coordinate. Despite the latter system benefits from a less destabilizing Pauli repulsion, particularly at the transition state region, the remaining attractive interactions are clearly stronger for the process involving the parent C_{60}-fullerene. For instance, at the same C···C forming distance of 2.3 Å, the computed ΔV_{elstat} = −39.9 kcal/mol and ΔE_{orb} = −40.7 kcal/mol values for the reaction involving $C_{59}NH$ are comparatively lower (i.e., weaker) than the respective values computed for C_{60} (ΔV_{elstat} = −47.5 kcal/mol and ΔE_{orb} = −53.0 kcal/mol). In addition, the latter system also benefits from stronger dispersion interactions, albeit to a much lesser extent ($\Delta\Delta E_{disp}$ = 2.5 kcal/mol). Therefore, it can be concluded that the stronger interaction between the deformed reactants computed for the cycloaddition between CP and C_{60}, which is translated into a lower activation barrier, finds its origin mainly in the stronger orbital and electrostatic interactions between the reactants practically along the entire reaction coordinate.

Finally, the orbital interactions, ΔE_{orb}, given by the EDA method can be further quantitatively partitioned by using the NOCV (Natural Orbital for Chemical Valence) extension of the EDA method.[22] Thus, the EDA-NOCV approach suggests that two main molecular orbital interactions dominate the total orbital interactions in these processes, namely the π(diene)→π^*(fullerene) and the reverse π(fullerene)→π^*(diene) interactions (see Figure 4, charge flow is red → blue). The former interaction is, as expected for a normal electronic demand DA process, clearly higher than the reverse interaction (i.e., $\Delta E(\rho_1) > \Delta E(\rho_2)$). Strikingly, both orbital interactions are clearly stronger for the process involving C_{60} than for $C_{59}NH$ (see Figure 4 for the interactions occurring at the same C···C distance of ca. 2.3 Å). Therefore, it can be concluded that the stronger orbital interactions in the parent C_{60}-fullerene, which leads to an enhanced DA reactivity as compared to its azafullerene counterpart, derive mainly from a stronger π(diene)→π^*(fullerene) interaction, but also from a stronger reverse π(fullerene)→π^*(diene), albeit to a much lesser extent.

In conclusion, we have computationally analyzed the factors controlling the DA reactivity of $C_{59}NH$-azafullerene in

DOI: 10.1021/acs.joc.6b02424
J. Org. Chem. 2017, 82, 754–758

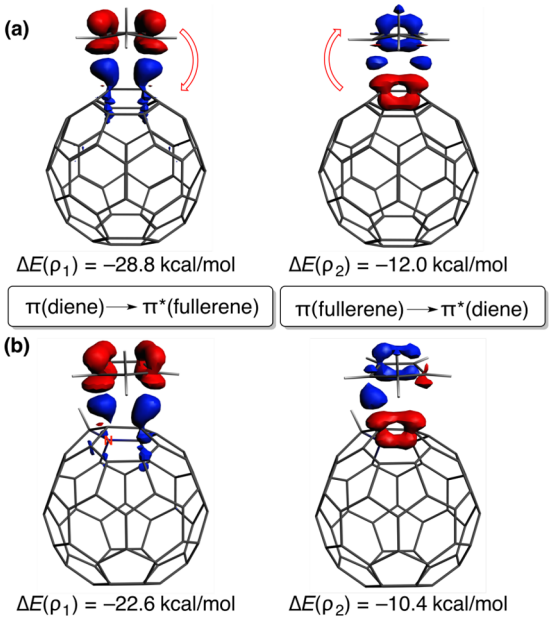

Figure 4. Plot of the deformation densities ($\Delta\rho$) of the pairwise orbital interactions between CP and C_{60} (a) and $C_{59}NH$ (b) and associated stabilization energies (ΔE, in kcal/mol). The color code of the charge flow is red → blue.

comparison with the parent C_{60}-fullerene. Besides predicting the regioselectivity of the transformation, the reduced reactivity of the $C_{59}NH$ system has been quantitatively analyzed in detail. It is found that the presence of the nitrogen atom and the CH fragment in the fullerene strongly modifies the nature of the cage in the sense that the interaction between the deformed reactants along the reaction coordinate is remarkably reduced. This weaker interaction is mainly the result of weaker electrostatic and orbital interactions, the latter coming mainly from a lower π(diene)→π*(fullerene) interaction. We believe that the insight gained in this study will guide further experimental developments in the less explored chemistry of heterofullerenes.

■ ASSOCIATED CONTENT

Supporting Information

The Supporting Information is available free of charge on the ACS Publications website at DOI: 10.1021/acs.joc.6b02424.

Figures S1 and S2 (showing the computed profile involving the most reactive bond of $C_{59}N$), computational details and Cartesian coordinates and energies of all species discussed in the text (PDF)

■ AUTHOR INFORMATION

Corresponding Author

*E-mail: israel@quim.ucm.es.

ORCID

Miquel Solà: 0000-0002-1917-7450

Israel Fernández: 0000-0002-0186-9774

Notes

The authors declare no competing financial interest.

■ ACKNOWLEDGMENTS

We are grateful for financial support from the Spanish MINECO-FEDER (Grants CTQ2013-44303-P, CTQ2016-78205-P, and CTQ2014-51912-REDC to I.F. and CTQ2014-54306-P to M.S.), Fundación BBVA (Convocatoria 2015 de Ayudas Fundación BBVA a Investigadores y Creadores Culturales), and Catalan DIUE (Projects 2014SGR931, ICREA Academia 2014 prize, and XRQTC to M.S.). The FEDER Grant UNGI10-4E-801 has also funded this research. Y.G.-R. acknowledges the MINECO for a FPI grant.

■ REFERENCES

(1) (a) *Fullerenes: From Synthesis to Optoelectronic Properties*; Guldi, D. M., Martín, N., Eds.; Kluwer: Dordrecht, 2002. (b) *Fullerenes. Principles and Applications*; Langa, F., Nierengarten, J.-F., Eds.; RSC: Cambridge, 2011. (c) Martín, N. *Chem. Commun.* **2006**, 2093.

(2) Kroto, H. W.; Heath, J. R.; O'Brien, S. C.; Curl, R. F.; Smalley, R. E. *Nature* **1985**, *318*, 162.

(3) Hirsch, A.; Bettreich, M. *Fullerenes, Chemistry and Reactions*; Wiley-VCH: Weinheim, 2005.

(4) Vostrowsky, O.; Hirsch, A. *Chem. Rev.* **2006**, *106*, 5191.

(5) (a) Hummelen, J. C.; Knight, B.; Pavlovich, J.; González, R.; Wudl, F. *Science* **1995**, *269*, 1554. (b) Nuber, B.; Hirsch, A. *Chem. Commun.* **1996**, 1421.

(6) Hashikawa, Y.; Murata, M.; Wakamiya, A.; Murata, Y. *J. Am. Chem. Soc.* **2016**, *138*, 4096.

(7) (a) Keshavarz-K, M.; González, R.; Hicks, R. G.; Srdanov, G.; Srdanov, V. I.; Collins, T. G.; Hummelen, J. C.; Bellavia-Lund, C.; Pavlovich, J.; Wudl, F.; Holczer, K. *Nature* **1996**, *383*, 147. (b) Xin, N.; Huang, H.; Zhang, J.; Dai, Z.; Gan, L. *Angew. Chem., Int. Ed.* **2012**, *51*, 6163. For a recent review, see (c) Rotas, G.; Tagmatarchis, N. *Chem. - Eur. J.* **2016**, *22*, 1206.

(8) (a) Zhang, G.; Huang, S.; Xiao, Z.; Chen, Q.; Gan, L.; Wang, Z. *J. Am. Chem. Soc.* **2008**, *130*, 12614. (b) Neubauer, R.; Heinemann, F. W.; Hampel, F.; Rubin, Y.; Hirsch, A. *Angew. Chem., Int. Ed.* **2012**, *51*, 11722.

(9) (a) Martin-Gomis, L.; Rotas, G.; Ohkubo, K.; Fernández-Lazaro, F.; Fukuzumi, S.; Tagmatarchis, N.; Sastre-Santos, A. *Nanoscale* **2015**, *7*, 7437. (b) Rotas, G.; Charalambidis, G.; Glatzl, L.; Gryko, D. T.; Kahnt, A.; Coutsolelos, A. G.; Tagmatarchis, N. *Chem. Commun.* **2013**, *49*, 9128.

(10) Representative examples: (a) Osuna, S.; Swart, M.; Solà, M. *Chem. - Eur. J.* **2009**, *15*, 13111. (b) Garcia-Borràs, M.; Osuna, S.; Luis, J. M.; Swart, M.; Solà, M. *Chem. - Eur. J.* **2012**, *18*, 7141. (c) Garcia-Borràs, M.; Osuna, S.; Swart, M.; Luis, J. M.; Solà, M. *Chem. Commun.* **2013**, *49*, 1220.

(11) For recent reviews, see: (a) Fernández, I.; Bickelhaupt, F. M. *Chem. Soc. Rev.* **2014**, *43*, 4953. (b) Wolters, L. P.; Bickelhaupt, F. M. *WIREs Comput. Mol. Sci.* **2015**, *5*, 324.

(12) von Hopffgarten, M.; Frenking, G. *WIREs Comput. Mol. Sci.* **2012**, *2*, 43 and references therein.

(13) (a) Fernández, I.; Solà, M.; Bickelhaupt, F. M. *Chem. - Eur. J.* **2013**, *19*, 7416. (b) Fernández, I.; Solà, M.; Bickelhaupt, F. M. *J. Chem. Theory Comput.* **2014**, *10*, 3863. (c) Bickelhaupt, F. M.; Solà, M.; Fernández, I. *Chem. - Eur. J.* **2015**, *21*, 5760. (d) García-Rodeja, Y.; Solà, M.; Bickelhaupt, F. M.; Fernández, I. *Chem. - Eur. J.* **2016**, *22*, 1368. (e) García-Rodeja, Y.; Solà, M.; Fernández, I. *Chem. - Eur. J.* **2016**, *22*, 10572.

(14) For very recent studies: (a) Lou, N.; Li, Y.; Cui, C.; Liu, Y.; Gan, L. *Org. Lett.* **2016**, *18*, 2236. (b) Eigler, R.; Heinemann, F. W.; Hirsch, A. *Chem. - Eur. J.* **2016**, *22*, 13575.

(15) All calculations were carried out at the ZORA-BP86-D3/TZ2P+//RI-BP86-D3/def2-SVP level. This level was chosen because it was confirmed to provide accurate activation and reaction energies for the parent cycloaddition between C_{60} and cyclopentadiene (see refs 13a and 16). See Computational Details in the Supporting Information.

(16) (a) Osuna, S.; Swart, M.; Solà, M. *J. Phys. Chem. A* **2011**, *115*, 3491. (b) Garcia-Borràs, M.; Luis, J. M.; Swart, M.; Solà, M. *Chem. - Eur. J.* **2013**, *19*, 4468.

DOI: 10.1021/acs.joc.6b02424
J. Org. Chem. 2017, 82, 754−758

(17) Calculations in the presence of toluene as solvent indicate that the solvent effect in this process is negligible ($\Delta E^{\ddagger}$ = 7.7 kcal/mol and ΔE_R = − 21.1 kcal/mol).
(18) A similar result was found previously by using much less accurate AM1 calculations. However, the predicted regioselectivity is completely different. See: Liang, Y.; Shang, Z.; Xu, X.; Zhao, X. *Acta Phys. − Chim. Sin.* **2008**, *24*, 1811.
(19) (a) Ess, D. H.; Houk, K. N. *J. Am. Chem. Soc.* **2007**, *129*, 10646. (b) Ess, D. H.; Houk, K. N. *J. Am. Chem. Soc.* **2008**, *130*, 10187. (c) Medina, J. M.; Mackey, J. L.; Garg, N. K.; Houk, K. N. *J. Am. Chem. Soc.* **2014**, *136*, 15798.
(20) (a) Fernández, I.; Bickelhaupt, F. M. *J. Comput. Chem.* **2014**, *35*, 371. (b) García-Rodeja, Y.; Fernández, I. *J. Org. Chem.* **2016**, *81*, 6554.
(21) (a) Fernández, I.; Bickelhaupt, F. M.; Cossío, F. P. *Chem. - Eur. J.* **2009**, *15*, 13022. (b) Fernández, I.; Cossío, F. P.; Bickelhaupt, F. M. *J. Org. Chem.* **2011**, *76*, 2310. (c) Fernández, I.; Bickelhaupt, F. M.; Cossío, F. P. *Chem. - Eur. J.* **2012**, *18*, 12395. (d) Fernández, I.; Bickelhaupt, F. M.; Cossío, F. P. *Chem. - Eur. J.* **2014**, *20*, 10791. (e) Fernández, I. *Phys. Chem. Chem. Phys.* **2014**, *16*, 7662. (f) Fernández, I.; Cossío, F. P. *J. Comput. Chem.* **2016**, *37*, 1265.
(22) Mitoraj, M. P.; Michalak, A.; Ziegler, T. *J. Chem. Theory Comput.* **2009**, *5*, 962.

DOI: 10.1021/acs.joc.6b02424
J. Org. Chem. 2017, 82, 754−758